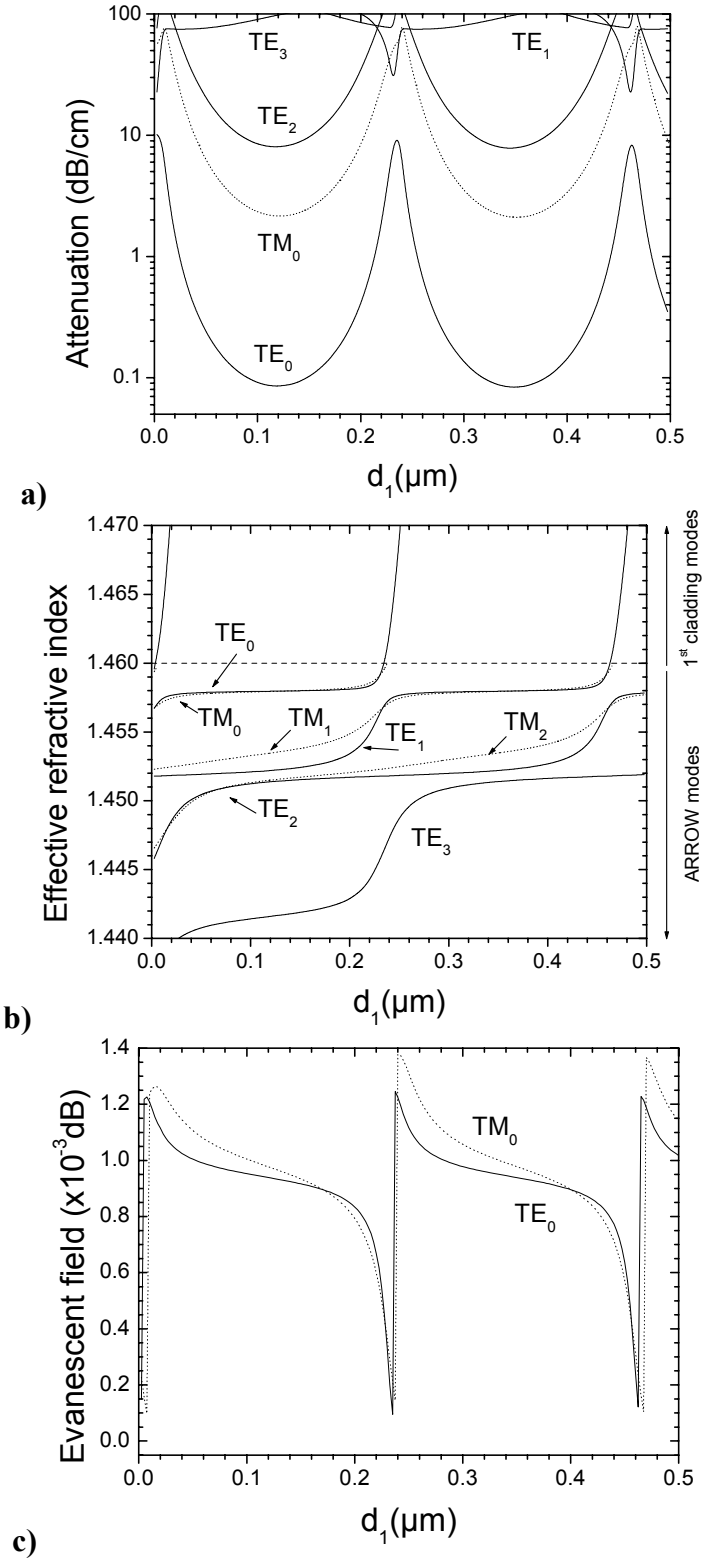

Fig 2.7.: Attenuation (a), dispersion (b) and evanescent field (c) for the lower TE and TM modes vs. d_1 for ARROW-A structures. Parameters were the same as in fig 2.6, except that d_2 was fixed at 2.0 μm.

Then, the ARROW-B modes have the highest effective refractive index of the whole structure. As the 1st cladding layer gets thicker, the overall structure tends to behave as a standard TIR waveguide, since the configuration obtained would be a core surrounded by both sides with thick layers having lower refractive index. This fact implies that ARROW-B structures must be carefully designed, because if the 1st cladding layer is not thin enough, it could be possible to have a multimode configuration. That is, the change in the structure confinement properties, from antiresonance to TIR. In ARROW-B structures there is no modal transition. Then, it is logical that above a certain value of d_1, the increase of the first cladding layer does not cause variations on the confining properties except a decrease of the attenuation of all modes, since the evanescent tail of the higher modes will not reach the absorbing substrate. Concerning the polarization, it can also be seen that TM_0 mode has a slight higher evanescent field as compared to TE_0. Since the former has a high attenuation and lower effective refractive index, it is no so good confined and thence, the evanescent field of the TM_0 mode has to be higher than these of the TE_0.

So far, it has been possible to optimize the antiresonant layers so as to obtain minimum attenuation losses. It also has been observed that, although TM modes have higher losses, its behavior is exactly the same as TE modes. It could had been predicted, since the single difference between both polarization on the antiresonant confinement is the different Fresnel reflection coefficient, being the lowest for TM.

In the previous section, a discussion was made concerning which factors were involved in the waveguide behavior as the core thickness was progressively decreased. In fig. 2.9 the attenuation (a) and the evanescent field (b) as a function of d_c can be observed. As expected, increasing the core thickness causes a major adaptation of the light inside the waveguide and a reduction of the evanescent field. If the mode is more confined, the decrease of the losses is straightforward. Again, this behavior is exactly the same for TE and TM polarization, although the latter has higher losses. At this point, it becomes clear the reason why choosing a 4μm core thickness.

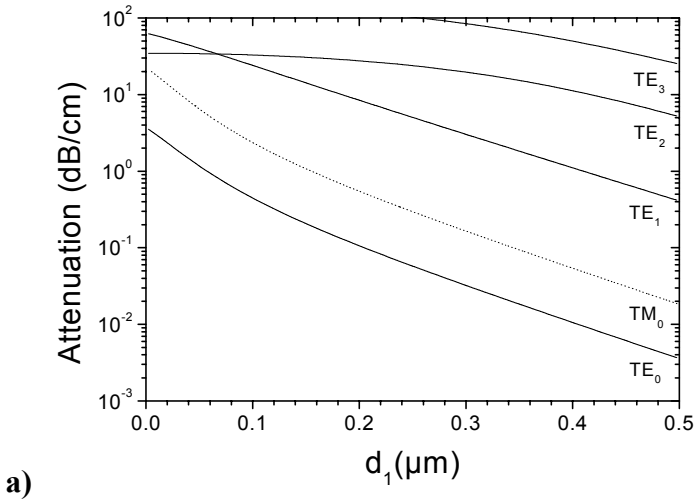

a)

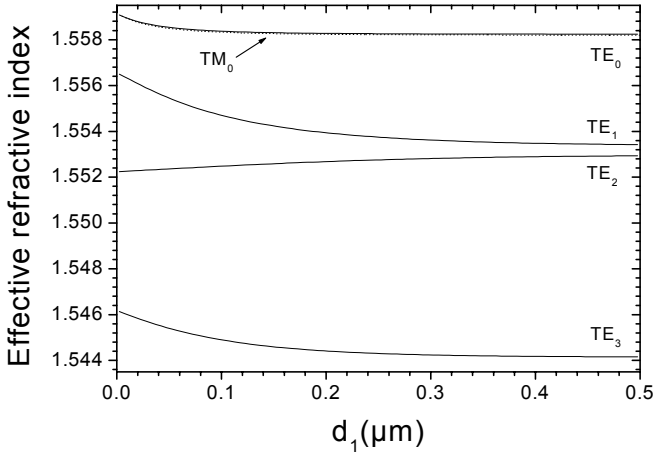

b)

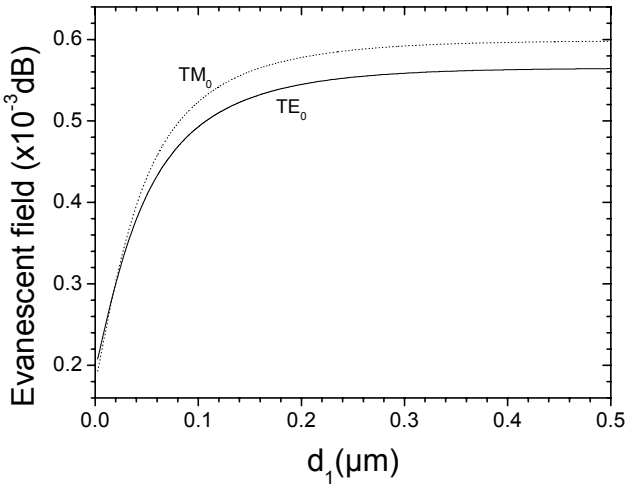

c)

Fig 2.8.: Attenuation (a), dispersion (b) and evanescent field (c) for the lower TE and TM modes vs. d_1 for ARROW-B structures. Parameters were the same as in fig 2.6, except that d_2 was fixed at 2 μm.

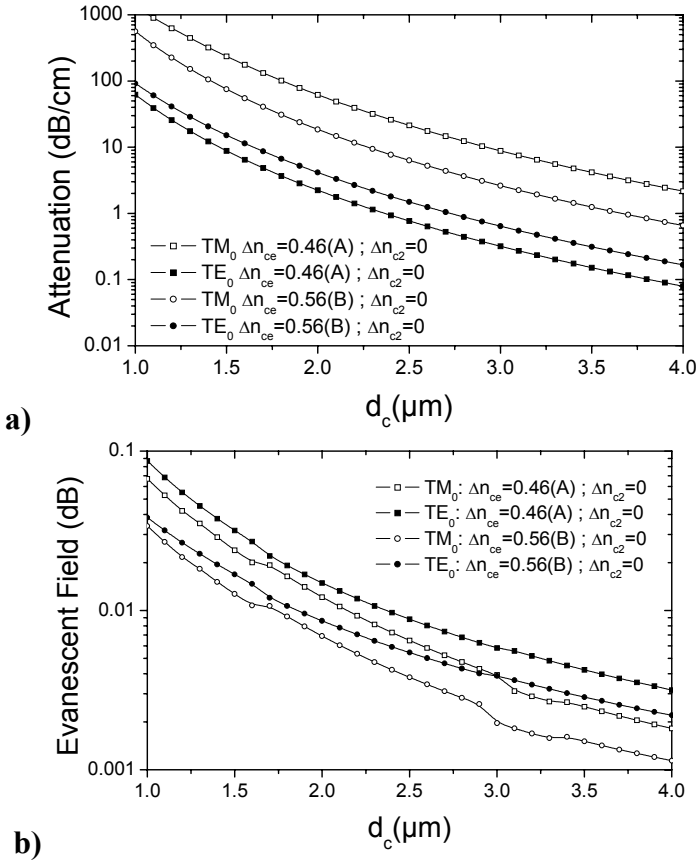

Fig 2.9.: Attenuation (a) and evanescent field (b) for the lower TE and TM modes vs. d_c for ARROW structures. For ARROW-A parameters were, $\Delta n_{c2}=0$, $\Delta n_{ce}=0.46(A)$, $d_2=d_c/2$ and d_1 was fixed in antiresonance. While $\Delta n_{c2}=0$, $\Delta n_{ce}=0.56(B)$, $d_2=d_c/2$ and $d_1=0.5\mu m$ were for ARROW-B.

Nowadays, there exist a wide variety of deposition systems that provide huge possibilities on obtaining different materials. These systems are, however, extremely complicated and there are several variables that have to be controlled during the deposition process. If any of these variables slightly changes its value, it could cause a change in the refractive index and/or the layer thickness. Although so far we know that antiresonant regions are wide enough to stand small thickness variations, it will be interesting knowing how ARROW configuration behaves when small variations on the refractive indexes are produced. In Fig. 2.10, the attenuation for ARROW-A (a) and ARROW-B (b) as a function of d_1 is presented for two different internal asymmetry parameters. As can be seen, for both structures, the attenuation of all modes decreases as Δn_{c2} increases. This fact is extremely important and has to be taken into account on the fabrication of any ARROW-based devices. A small difference on the refractive

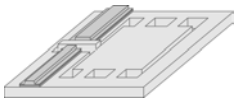

index between the core and the second cladding layer causes a overall decrease on the attenuation for all modes of the waveguide, causing the structure to have a multimode behavior. This fact can be clarified considering the refractive index profile of both structures. If the core has a slightly higher refractive index as compared to the second cladding layer, since d_1 has been designed to be thin enough so as to permit that the mode tail reaches the second cladding layer, a standard TIR configuration would be obtained. Hence, although d_1 still works in the antiresonant configuration, the waveguide would have a multimode behavior. Thus, it could be said that the internal asymmetry parameter is the main responsible of the number of guided modes in the ARROW structure.

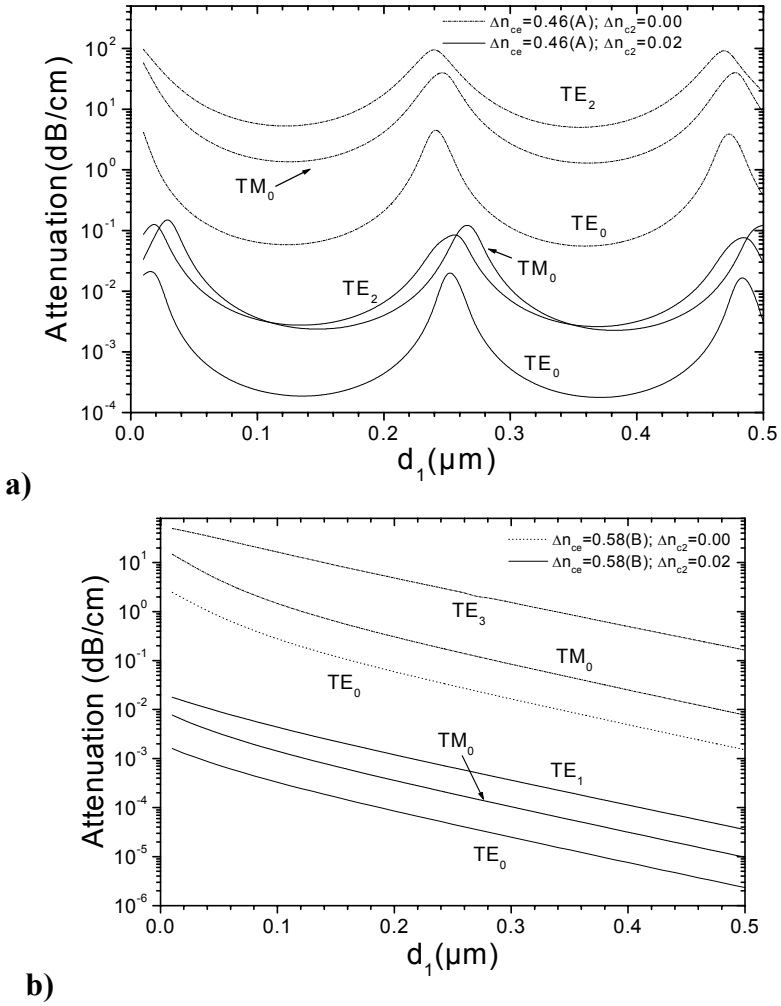

Fig 2.10.: Attenuation as a function of d_1 for both polarization and two Δn_{c2} values in ARROW-A (a) and ARROW-B (b) structures. Parameters were the same as in fig 2.6.

The effects of the external asymmetry parameter on the optical properties of ARROW structures has also been studied. In fig. 2.11a the attenuation for an ARROW-A structure as a function of Δn_{ce} for the three lowest order modes of both polarizations can be observed. For this simulation, d_1 was tuned in antiresonance for the TE_0 according to the parameters involved, and $d_c = 2d_2 = 4\mu m$. It could be thought that the attenuation should increase as Δn_{ce} was lower, since the confinement in the waveguides would be lower. Although this assumption could be considered as appropriate for values below $\Delta n_{ce}=0.6$, the increase of the attenuation for large Δn_{ce} values cannot be explained under this approach. If field amplitude for different Δn_{ce} is plotted (fig. 2.11b) it can be seen that as Δn_{ce} increases, at the upper boundary layer the TIR-based confinement increases, while it happens the contrary with the antiresonant-based confinement on the lower boundary layer. Hence, there exists a competence between both types of confinement: For large Δn_{ce} values, the high refractive index difference at the upper layer causes a strong confinement. However, the small refractive index difference between the core and the first cladding layer also causes the interference cladding to be weak. On the contrary, for $\Delta n_{ce} \rightarrow 0$, the evanescent tail in the external media is the highest due to a low confinement factor at that boundary layer. At the lower interface the confinement is maximum, since the refractive index difference is the highest.

The behavior of ARROW-B structures as a function of the external asymmetry can be seen in fig. 2.12. Both attenuation (2.12a) and field amplitude profile (2.12b) behaves significantly different as compared to ARROW-A structures. This fact can be mainly associated to the fact that n_1 is the lowest in the overall structure. As previously commented, if d_1 is excessively thick, ARROW-B will have a multimode configuration. Now, according to the attenuation monotonous decrease of fig. 2.12a, a new limitation can be stated: If the external asymmetry parameter is excessively large for a given d_1, several modes would have low attenuation losses and multimode behavior would be obtained. The confirmation of this affirmation can be found in the field amplitude profiles shown in fig. 2.12b. As Δn_{ce} increases, the evanescent tail propagating through d_1 fastly disappears, interferences are no longer produced at d_2 layer and ARROW-B modes are replaced by TIR-based modes.

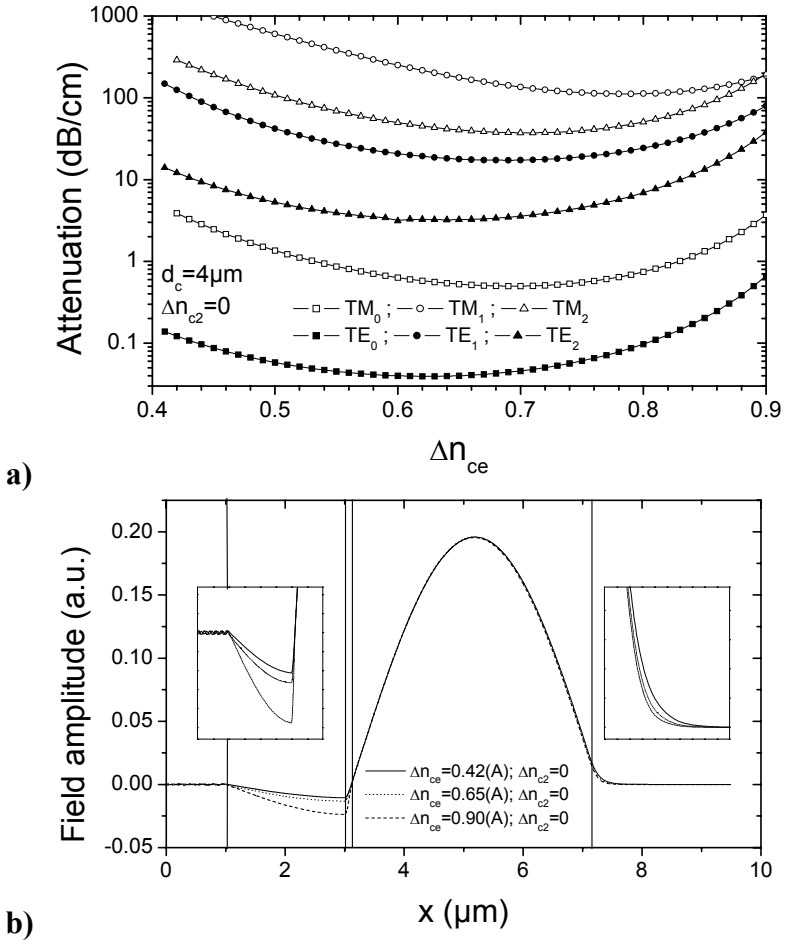

Fig 2.11.: a) Attenuation of the lowest three modes of an ARROW-A structure as a function of Δn_{ce} for both polarizations. b) TE_0 field amplitude profile for three different Δn_{ce} values.

Summing up, from all the previous simulations, it is possible to determine a region, shown in table 2.2, where optimum properties will be obtained both in ARROW-A and ARROW-B in terms of attenuation, confinement and modal properties.

	Δn_{ce}	Δn_{c2}	d_c (μm)	d_1 (μm)	d_2 (μm)
ARROW-A	0.45-0.75	0	3.5-4	0.08-0.14*	$d_c/2$
ARROW-B	0.50-0.60	0	3.5-4	0.3-0.5	$d_c/2$

* (2n+1) multiples of this value are also appropriate

Table 2.2: Optimal ARROW-A and ARROW-B working regions, according to the values obtained, for a fixed wavelength of 633nm.

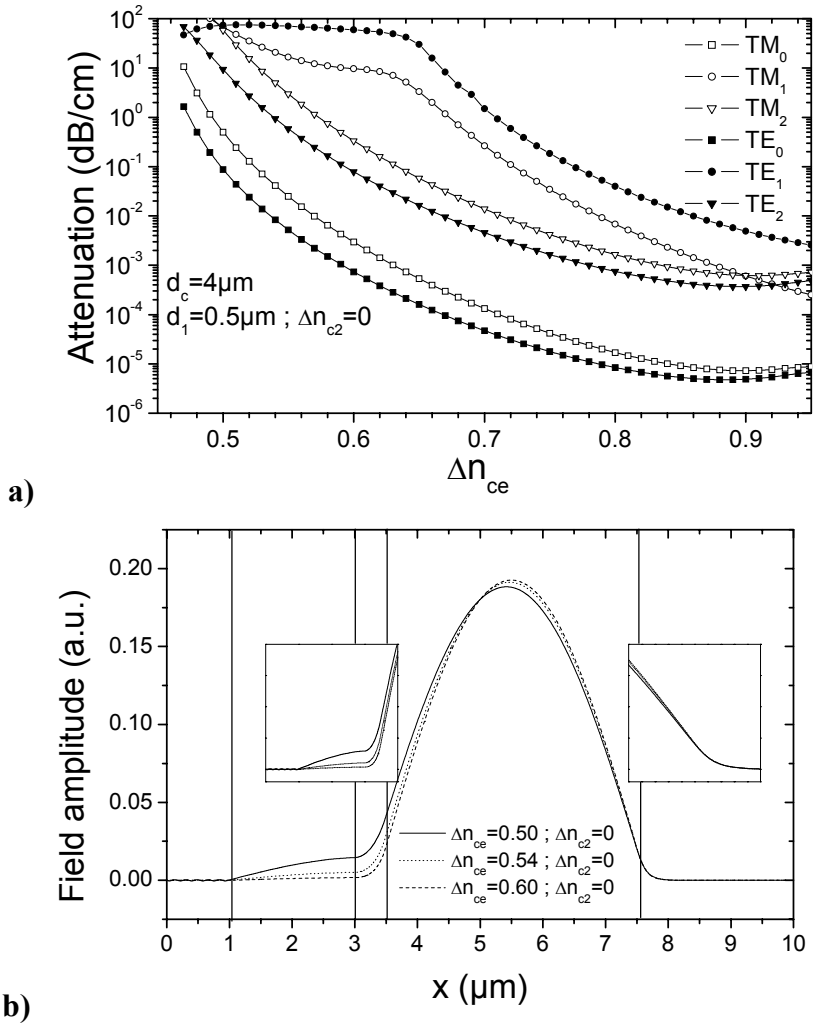

Fig 2.12.: a) Attenuation of the lowest three modes of an ARROW-B structure as a function of Δn_{ce} for both polarizations. b) TE_0 field amplitude profile for three different Δn_{ce} values.

2.3 Design of Passive Integrated Optical Devices

The previously studied slab structures have provided large information concerning the optical properties of ARROW-A and ARROW-B configurations. The direct application of these structures does not allow to design the major part of integrated optical devices. This is mainly due to the fact that there does not exist lateral confinement on the waveguides. What is commonly done is etch partially the core, as shown in fig. 2.13. Hence, confinement in the cross section (x,y) is obtained, being the light able to propagate only through the longitudinal dimension (z). Obviously, as the mode is confined on the non-etched core, the antiresonant properties remain unchanged.

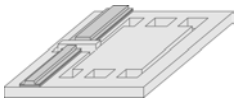

There are, however, changes on their modal properties. Etching the core allows having, apart from the previously studied ARROW modes, some lateral modes whose number will depend on the rib width (w) and height (h).

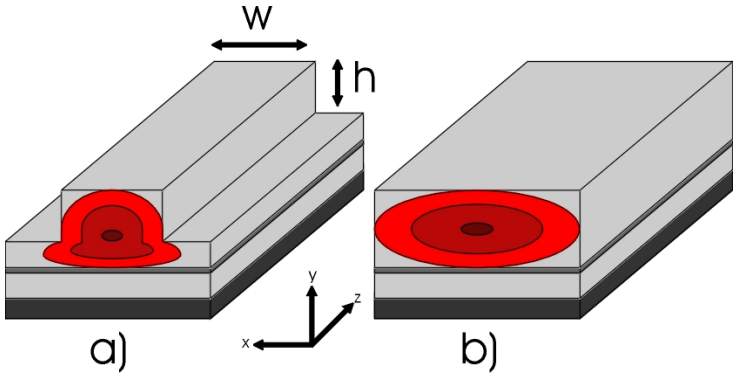

Fig 2.13.: a) Rib ARROW configuration that provides cross-section (x,y) confinement. b) Slab waveguide, were only confinement in y direction is achieved

An analysis of the lateral modal properties of ARROW-A structures has been done as a function of the rib height (h) for different widths (w). Results are shown in fig. 2.14. As it can be observed, there is a dramatic increase of the number of lateral modes as the rib or the width increases. This fact will be of extreme importance when designing passive devices. If the waveguide geometry is not accurately controlled, it could happen that a device thought to work under single-mode conditions actually have several longitudinal modes due to an excessive rib or width. ARROW-B lateral modes provide equivalent results and will not be shown, trying to avoid redundancy.

Nowadays, there exist a huge variety of passive optical devices that takes advantage of any/some properties of the light propagation to obtain the desired behavior. Actually, optical devices are, in general, much more flexible and adaptable than their electronic counterparts. Interference, diffraction, reflection, and some other light properties probably make them the most powerful devices in the field of sensors and telecommunications.

Although it could be detailed the different light optical properties and how to apply any of these to a concrete passive integrated optical device, we will restrict ourselves to three main properties that have been used in the fabrication of integrated optics devices: Power (or intensity), phase change and evanescent field.

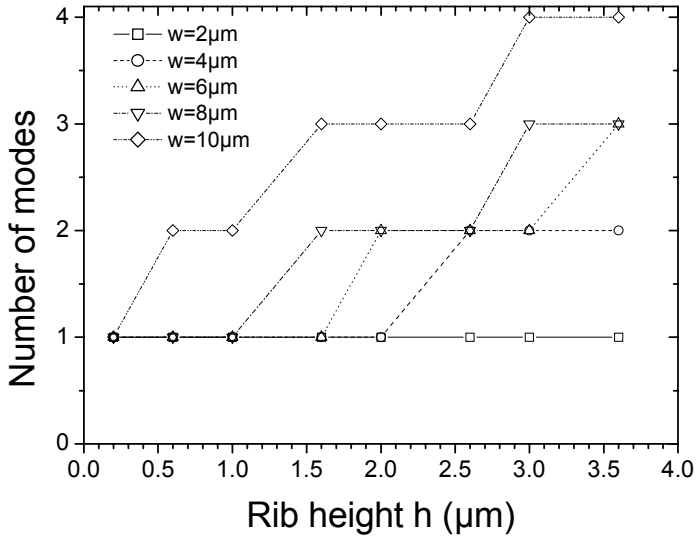

Fig 2.14.: Number of modes in an ARROW-A structure as a function of the rib height (h) for several waveguide widths

2.3.1 *Power Optical Devices*

Generally, any kinds of losses are undesirable in any optical device. There are, however, some configurations where a change in the total amount of power at the device output allows obtaining information about the light optical path. In this kind of devices, the modal properties are not important, but are the difference between the input and the output power. For that reason, we have labeled them as power optical devices.

Two different configurations of power optical devices have been proposed, as shown in fig. 2.15. The basic configuration consists in two waveguides with a free-space zone (FSZ) between them. When light coming from the input waveguide reaches the FSZ, it broadens due to beam broadening **[15]**. An output waveguide is placed at a certain distance so as to collect as maximum power as possible. In case a), an absorbent media is placed in the FSZ, causing a partial decrease or even a null power at the output. Knowing the power with the FSZ empty, the amount of power at the output when an absorbent media is placed in the FSZ will provide information concerning the absorbance properties of this media. In case b), on the contrary, no absorbent is placed in the FSZ. Now, the output waveguide has a displacement. Since waveguides are no longer head-to-head, part of the power is not collected. Under this configuration, the

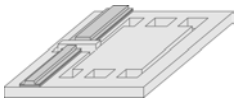

power at the output would provide information concerning the misalignment between waveguides.

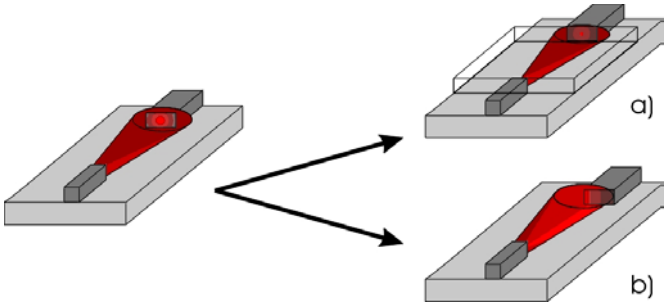

Fig 2.15.: Power optical configurations proposed a) with absorbent media between the waveguides. b) with misalignment of the input/output waveguides.

It could be said that on power optical devices, no single-mode properties are necessary, since the only parameter of interest is the amount of power at the output. Although this fact is completely true, it has to be noted that single-mode behavior is only one of the several properties of ARROW waveguides. The reason why also using these structures on this application is the capability of obtaining large core waveguides without using large buffer layers.

2.3.1.1 Chemical Application: Absorption Sensor

A very simple, however effective way of obtaining a chemical absorbance sensor is the deposition of a membrane on the FSZ. According to the Lambert-Beer law **[16]**, the ratio between the input intensity I_0 injected to a membrane and the intensity I at the output allows determining the absorbance (A) of a compound at a given wavelength:

$$A = Log\left(\frac{I}{I_0}\right) = C\varepsilon d \qquad (2.11)$$

where ε is the molar absorbity, C stands for the concentration of species to be measured and d is the optical path, that generally is the membrane length.

Properties of this membrane have to be accurate, stable and well known. Suppose that the intention is to quantify the amount of a certain composite, either diluted in a gas or in a liquid. The membrane should have the following properties: 1. Being completely transparent when the target composite is not present. 2. When a particle of target composite interacts with the membrane, it has to locally change its

properties. Depending on the amount of composite, the membrane properties should shift from transparency to complete opacity (it is also possible to work in the opposite conditions. That is, starting from opacity and heading towards transparency when target composites are present). Although it may seem too difficult a membrane with such a specific behavior, it has been designed, fabricated and deposited over the device with excellent results, as they will be shown in chapter 5. Deposition of this membrane is, however, a bottleneck, since it has to be done chip by chip, via a needle. Hence, the FSZ dimensions should be as big as possible so as to easy the membrane deposition.

Concerning the waveguides, it is necessary to choose which widths and rib should provide the best results. The confinement factor increases as the rib increases, but it will also increase the number of lateral modes. Since the modal properties are not important on power devices, a deep etch (3.5µm) over a 4µm core layer will be considered as optimum. Due to beam broadening, the second waveguide should be wider than the first. In fig. 2.16, a light beam coming from a 5µm width waveguide has been left to propagate freely.

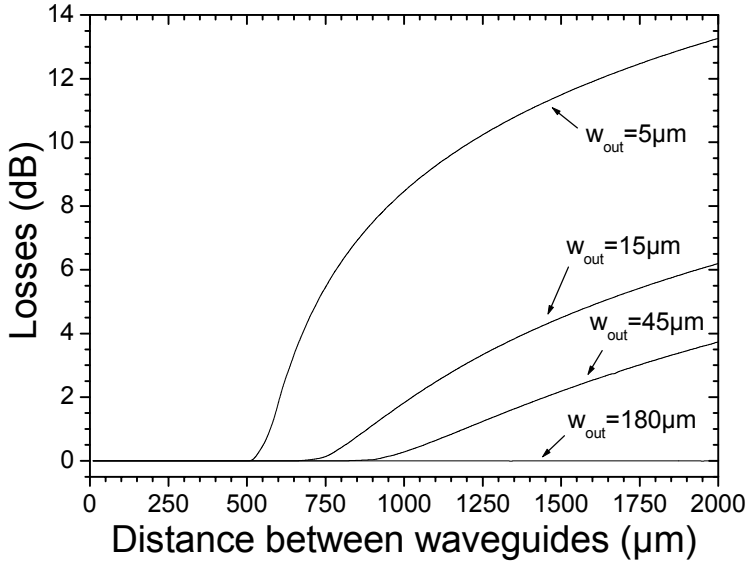

Fig 2.16.: Losses caused by beam broadening. The incoming light from a 5µm-width waveguide is launched into a free space zone and collected, after a given distance, into a wider waveguide.

At a given distance, a second waveguide was placed head-to-head. As can be seen, as this second waveguide widens, the amount of collected power increases. In our

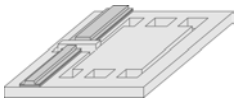

concrete application, it is required that the input waveguide to be relatively wide so as to easy the light coupling from a fiber optics. Simulations have been done in order to optimize the overall dimensions of the structure. It has been observed that, if the waveguide input and output width are 14μm and 50μm, respectively, at a distance of 500μm the losses are completely neglectable. Even at 1000μm, losses are a mere 0.1dB, which is clearly affordable.

2.3.1.2 Physical Application: Uniaxial Optical Accelerometers

The simplest way to understand an accelerometer is a spring-mass system. When an external force is applied to this system (as could be a gravitational field), the mass acts over the spring, causing this latter to be deformed, suffering from mechanical stresses.

Modelization equations are extremely simple as the system basically consists on a damped harmonic oscillator. Thus, its movement equation is:

$$\mathrm{m}\frac{\mathrm{d}^2\mathrm{x}}{\mathrm{dt}^2} + B\frac{dx}{dt} + kx = ma \tag{2.12}$$

where x stands for the displacement, B for the damping coefficient, k the spring constant m the mass and a the acceleration. From the previous equation, the following parameters can be defined:

$$S_m = \frac{m}{k} \tag{2.13}$$

$$\omega_n = \sqrt{k/m} \tag{2.14}$$

$$\zeta = \frac{B}{2\sqrt{km}} \tag{2.15}$$

Where S_m is the mechanical sensitivity, ω_n stands for the system natural (or resonance) frequency and ζ is the damping factor. Among the previous parameters, the resonant frequency perhaps is the most important, since it limits the bandwidth operation. In order to minimize the offset errors, accelerometers should work far from resonance **[17]**. For that reason, they are mainly designed so as to have the highest natural frequencies possible, allowing a wide bandwidth. As a general rule, the bandwidth is limited to $\omega_n/10$, but this factor strongly depends on the damping factor.